Indonesian Physical Review
Volume 08 Issue 03, September 2025
P-ISSN: 2615-1278, E-ISSN: 2614-7904

# Numerical Simulation of Mw 8.3 South Buru Fault Tsunamis with 3D Slip Evolution in Ambon

**Josephus Ronny Kelibulin[1,3,4*], Grimaldy Rooy Latumeten[1,2], Alexander Yosep Elake[1,3,4] Annamaintin Kobong Lebang[1,5]**

[1] *Physics Department, Faculty of Science and Technology, University of Pattimura, Ambon, Indonesia*
[2] *Oceanography Laboratory, Faculty of Science and Technology, University of Pattimura, Ambon, Indonesia*
[3] *Computasi Laboratory, Faculty of Science and Technology, University of Pattimura, Ambon, Indonesia*
[4] *Geophysics Laboratory, Faculty of Science and Technology, University of Pattimura, Ambon, Indonesia*
[5] *Electronic and Instrumentation Laboratory, Faculty of Science and Technology, University of Pattimura, Ambon, Indonesia*

*Corresponding Author's E-mail: josephus.kelibulin@lecturer.unpatti.ac.id*

**Article Info**

***Article info:***
*Received: 25-07-2025*
*Revised: 08-09-2025*
*Accepted: 22-09-2025*

***Keywords:***
*South Buru Fault; numerical modeling; tsunami run-up; tsunami inundation; Ambon coastal area*

***How To Cite:***
*J.R. Kelibulin, G.R. Latumeten, A.Y. Elake, and A.K. Lebang, "Numerical Simulation of Mw 8.3 South Buru faults Tsunamis with 3D Slip Evolution in Ambon", Indonesian Physical Review, vol. 8, no. 3, pp. 840-855, 2025.*

***DOI:***
*https://doi.org/10.29303/ipr.v8i3.541.*

**Abstract**

*This study investigates the tsunami hazard potential induced by the activity of the South Buru Thrust Fault on the coastal areas of Ambon City through two-dimensional (2D) numerical modelling using the COMCOT v1.7 software, while incorporating three-dimensional (3D) slip evolution from the fault scenario. The earthquake scenario was set at Mw 8.3 based on fault length, width, and slip potential estimates, representing an extreme seismic event in the region. By integrating 3D slip evolution into the 2D tsunami model, the approach accounts for spatial variations in vertical displacement along the fault plane, directly influencing tsunami generation and propagation. The simulation results show significant spatial variations in tsunami run-up heights and inundation zones, with maximum run-up recorded at Kapahaha (13.08 m, arrival time ~832 s) and Slamet Riyadi Port (12.02 m, arrival time ~786 s). In comparison, minimum values occurred in Ambon's northern and northeastern parts (<1 m). The affected area and inundation distance from the shoreline also vary, e.g., Kapahaha (12,813 m², 159 m) and Slamet Riyadi Port (414,158 m², 1,213 m). Areas experiencing the highest tsunami inundation are Latuhalat (>5 m), followed by Galala–Wayame–Laha (3–5 m) and Paso–Rumah Tiga–Hative Kecil (2–4 m). The distribution of tsunami waves is influenced by coastal morphology, wave direction, and the presence of bays and capes, which can either amplify or block waves. Further analysis highlights the effects of seafloor topography, coastal morphology, and wave propagation pathways on run-up heights and arrival times. These findings underscore the importance of considering multi-segment rupture models, 3D deformation, and coastal morphology in tsunami hazard assessments and contribute to more realistic, source-specific mitigation strategies in tectonically complex regions such as Ambon.*

## Introduction

Indonesia is an archipelagic country located in a complex tectonic setting resulting from the convergence of three major lithospheric plates: the Indo-Australian, Eurasian, and Pacific. The interactions among these plates place the Indonesian region, particularly the Maluku Islands, among the world's most seismically and volcanically active areas [1]. The Maluku region is characterized by numerous active fault systems, both onshore and offshore, that have the potential to generate significant earthquakes and associated tsunamis. A tsunami is defined as the displacement of a water column caused by an impulsive disturbance, typically resulting from sudden vertical displacement of the seafloor [2] or, in some cases, horizontal fault motion [ 3].

Tsunamis, classified as geophysical natural hazards [4], are long-wavelength gravity waves generated by seismic events such as fault ruptures, submarine landslides, volcanic eruptions, meteorite impacts, or explosions near the sea surface. Historical records, including the Catalogue of Tsunamis on the Western Shore of the Pacific Ocean compiled by Soloviev and Go [5] and other tsunami databases, indicate that more than 85 tsunami events occurred in the Maluku region between 1600 and 2015. During the same period, 210 tsunami events were documented across the Indonesian archipelago, suggesting that approximately 40% of all tsunamis in Indonesia occurred in the Maluku region. One active fault of particular concern is the South Buru Fault, which trends approximately west–east along the southern segment of Buru Island. Seismotectonic activity along this fault has been documented on multiple occasions, including a magnitude 5.0 earthquake in October 2023 in the Banda Sea, which was attributed to local fault movement in the area [6]. The fault is inferred to exhibit a strike-slip to oblique-slip kinematic regime, capable of producing seafloor deformation sufficient to generate a tsunami, particularly if associated with a high-magnitude seismic event.

Ambon City, the capital of Maluku Province, has a south-facing coastline, making it particularly vulnerable to tsunamigenic impacts generated by the South Buru Fault. The high population density and socio-economic infrastructure concentration along Ambon Bay's coastal zone further increase the potential disaster risk [7]. However, to date, few studies have specifically modelled tsunami hazards and coastal inundation scenarios originating from this fault source, particularly regarding the coastal areas of Ambon City. Previous studies have modelled tsunamis on the eastern segment of the South Buru Fault to explain that the large tsunami that struck Ambon's coastal areas and its surroundings was likely triggered by a submarine landslide induced by an earthquake. In contrast, the western segment has not yet been modelled [8]. This study was designed to address three main objectives: to describe the characteristics of tsunami wave propagation resulting from tectonic activity along the South Buru Fault zone; to estimate the tsunami run-up height in the coastal areas of Ambon City under local earthquake source scenarios; and to identify the extent of tsunami impact zones based on numerical simulation results using local geological and seismic parameters.

Tsunami wave dynamics are strongly influenced by ocean depth. In deep water, wave speeds can reach 500 to 1,000 km/h, although wave heights remain relatively small, typically ranging from a few centimeters to several meters [9]. As the wave approaches the coastline, the decreasing depth causes the wave speed to drop to around 50 km/h. This deceleration is accompanied by a significant increase in wave height due to the accumulation of water mass, a phenomenon known as the shoaling effect [10]. In addition to depth and velocity, coastal morphology is crucial in influencing run-up processes, particularly in determining the inland

extent and elevation to which seawater intrudes. Gently sloping coastlines produce greater run-up elevations than steeper ones [11]. Laboratory experiments have shown that submerged structures, such as breakwaters, reduce run-up heights by up to 50% [12].

The methodology employed in this study is two-dimensional (2D) numerical modelling of tsunami propagation using the Shallow Water Equations (SWE) approach. This method simulates the tsunami wave dynamics from the source region near the South Buru Fault to the coastal areas of Ambon City. The primary steps include: (1) identifying and characterizing the tsunami source based on seismotectonic data and regional geological models; (2) simulating wave propagation using COMCOT software with parameters calibrated to various earthquake magnitude scenarios; and (3) analyzing the simulation outputs, including estimated run-up heights, wave arrival times, and the extent of inundation in potentially affected areas.

Compared to previous studies, which have predominantly focused on megathrust earthquake sources in the Banda and Seram Sea subduction zones [13],[14],15], this research presents several novel contributions. These include focusing on the tsunami potential generated by nearby fault activity—particularly the South Buru Fault, which is classified as a strike-slip to oblique-slip fault—and integrating region-specific geological and seismic data to develop more accurate source scenarios. Additionally, this study includes a spatial analysis of tsunami impacts in Ambon City, which serves as the economic and population centre of Maluku Province.

Through this approach, the research aims to contribute to improved tsunami hazard assessments based on local sources in eastern Indonesia and to support the formulation of science-based disaster mitigation policies. This study selected a maximum credible earthquake magnitude of Mw 8.3 for the South Buru Fault scenario. This value was determined based on the fault's estimated rupture length, width, and slip potential, collectively indicating its capability to generate an extreme seismic event. Using this upper-bound magnitude ensures that the simulations represent the worst-case scenario for regional tsunami hazard assessment. However, modelling tsunami hazards generated by non-subduction sources, such as local thrust and strike-slip faults, presents specific challenges compared to megathrust earthquakes. These challenges include the relatively limited historical records, greater uncertainties in fault parameters, and the complex influence of segmentation on tsunami generation. These issues underscore the importance of considering non-subduction sources in tsunami assessments for eastern Indonesia. The study area, including the South Buru Fault zone, is illustrated in Figure 1.

## Method

To evaluate tsunami hazards from the South Buru Fault, 2D simulations using COMCOT v1.7 were conducted. This section outlines the method used to model tsunami generation, propagation, and run-up based on a hypothetical Mw 8.3 earthquake and 3D slip evolution.

### Numerical Simulation Method

The research methodology in this study involves several interrelated stages. The first stage focuses on a numerical approach using the COMCOT v1.7 software. Tsunami waves possess stable and continuous energy that propagates momentum in all directions, not only on the surface but also downward, encountering bottom friction. The COMCOT model applies a

nonlinear Shallow Water Equations (SWE) approach using a leap-frog finite difference scheme [16],[17], as illustrated in the grid sketch in Figure 2.

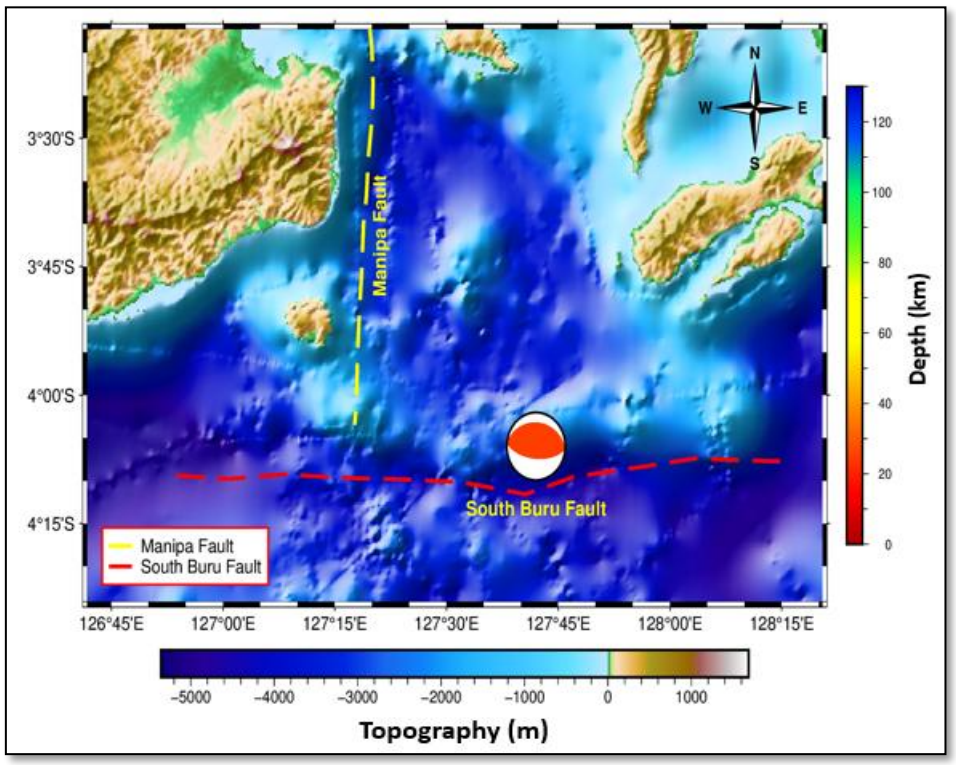


**Figure 1.** Research location in the South Buru Fault

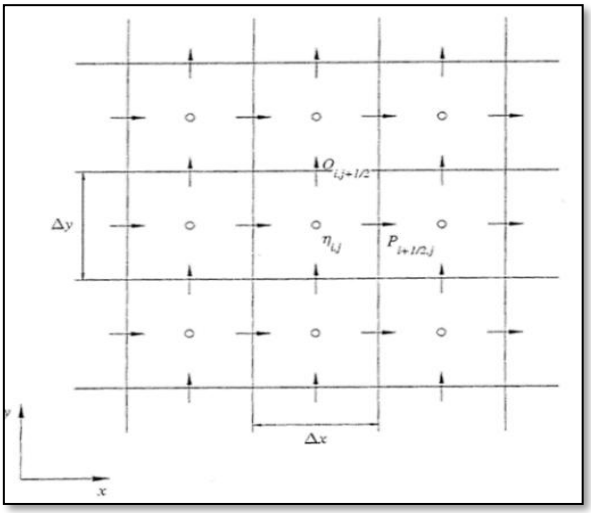


**Figure 2**. Sketch of the COMCOT Builder Grid [17]

In solving the shallow water equations in both spherical and Cartesian coordinates, COMCOT v1.7 adopts a leap-frog numerical scheme. The tsunami simulation in this study

uses nonlinear equations in spherical coordinates, incorporating bottom friction effects to represent flow behaviour as it enters shallow coastal areas [18],[19]. The nonlinear shallow water equations and bottom friction terms used in the spherical coordinate system [17] are expressed as follows:

$$\frac{\partial \eta}{\partial t} + \left\{\frac{\partial P}{\partial x} + \frac{\partial Q}{\partial y}\right\} = -\frac{\partial h}{\partial t} \quad (1)$$

$$\frac{\partial P}{\partial t} + \frac{\partial}{\partial x}\left\{\frac{P^2}{H}\right\} + \frac{\partial}{\partial y}\left\{\frac{PQ}{H}\right\} + gH\frac{\partial \eta}{\partial x} + F_x = 0 \quad (2)$$

$$\frac{\partial Q}{\partial t} + \frac{\partial}{\partial x}\left\{\frac{PQ}{H}\right\} + \frac{\partial}{\partial y}\left\{\frac{Q^2}{H}\right\} + gH\frac{\partial \eta}{\partial y} + F_y = 0 \quad (3)$$

$$F_x = \frac{gn^2}{H^{\frac{7}{3}}} P(P^2 + Q^2)^{\frac{1}{2}} \quad (4)$$

$$F_y = \frac{gn^2}{H^{\frac{7}{3}}} Q(P^2 + Q^2)^{\frac{1}{2}} \quad (5)$$

Where: H (h + η) represents total water depth (m); P and Q are fluxes in the x and y directions ($m^2/s$); g is the acceleration due to gravity ($m/s^2$); Fx and Fy denote bottom friction in the x and y directions; and n is the Manning's roughness coefficient. The friction coefficient used in this study follows Manning's formulation, set at 0.0013 across all simulation layers. This coefficient may be applied uniformly or vary per simulation layer [19],[20]. The data required for analyzing the areas affected by the tsunami consists of bathymetric data from the GEBCO (General Bathymetric Chart of the Ocean), topographic data for reviewing the regions affected by the tsunami in the form of DEM (Digital Elevation Model Data) using Global Mapper, and earthquake and tsunami data from BMKG.

**Scenario Design and Model Simulation**

Scenarios were developed to simulate tsunami hazards along the Ambon coast using fault parameters derived from the geological setting of the South Buru Fault. Table 1 summarises the spatial domain and model resolution used in the simulation, along with the key coordinates and grid size. These parameters are crucial for estimating tsunami run-up at selected coastal locations.

**Table 1.** Configuration of simulation scenario, grid size, and coordinate setup used in tsunami modeling from the South Buru Fault.

| Scenario Name | Grid Size (m) | Grid Dimension (NX×NY) | Coordinate X_start | Coordinate Y_start |
|---|---|---|---|---|
| South Buru Fault | 0.5 | 219 × 150 | 126.5853 | -4.5688 |

The simulation will be carried out based on several scenarios estimated from potential earthquake sources that could affect the coastal areas of Ambon Island. The estimation of earthquake parameters is derived from the geological conditions of the study area. The

location data of measurement points is essential to determine the tsunami run-up heights at those locations.

The tsunami simulation model will be conducted using a fault source located in the Seram Trough, with one different scenario applied. This fault source estimates the tsunami simulation, enabling the determination of key parameters such as wave height and arrival time. The parameters of the tsunami-generating fault include several critical components (Figure 3).

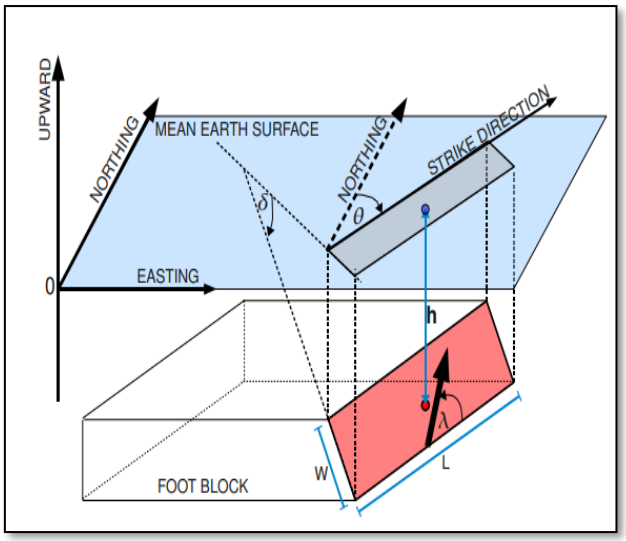


**Figure 3**. Fault parameters of a tsunami source [16]

The fault dimensions, consisting of width (W) as the vertical extent and length (L) as the horizontal extent of the rupture area, are specified. The fault coordinates, representing the location of the epicentre projected onto the surface, are also identified. Additional fault parameters include the focal depth (h), strike angle (θ), dip angle (δ), slip (m), rake angle (λ), and magnitude. The strike (θ) refers to the orientation of the fault line with respect to the north, the dip (δ) describes the inclination of the fault plane from the horizontal, and the rake angle (λ) indicates the direction of fault slip. Finally, the displacement or dislocation on the fault surface is also a crucial factor in the simulation.

## Result and Discussion

### Deformation Analysis and Its Implications for Tsunami Generation

The vertical deformation model resulting from the South Buru Thrust Fault activity demonstrates the classic characteristics of a thrust fault mechanism, where uplift occurs on the hanging wall and subsidence on the footwall side of the fault plane. The placement of the hypocenter precisely between the two deformation zones, as depicted in the model visualization, is a reasonable approach because it reflects the central source region of seismic energy release within the fault zone [20]. Uplift zones located near or beneath the seafloor are particularly significant in generating tsunamis, as they can displace a large column of water vertically and suddenly, triggering wave formation within seconds.

This type of vertical deformation is a primary indicator of the mechanisms that generate tsunamis. In the case of the South Buru Thrust Fault, the uplift occurs on the western segment of the fault (towards the Banda Sea), while the subsidence lies on the eastern side (in the direction of Buru Island). This suggests a substantial vertical energy transfer into the water column. Several studies indicate that uplift zones with vertical displacements ≥1 meter beneath the seafloor have a high potential to generate tsunamis with significant amplitudes [21],[22]. In other words, if the vertical displacement from fault rupture reaches several meters over a wide area, the amount of energy transferred to the ocean surface may result in dangerously high tsunami waves along the coast.

The geological conditions surrounding the South Buru Fault further support this scenario for a tsunami. This fault is part of a complex active subduction system in Eastern Indonesia and possesses a seismic history that is not yet fully documented. Although it is not part of the major megathrust systems, such as those in Sumatra or the Sunda arc, this thrusts fault can potentially generate large-magnitude earthquakes (Mw> 7.5–8.3), capable of triggering both local and regional tsunamis. The amplification of tsunami waves along coastal areas would also depend on factors such as bathymetry, earthquake depth, and the proximity of the rupture zone to the coastline. As explained by Geist and Parsons [23], shallow offshore thrust earthquakes (<20 km depth) with significant vertical slip components tend to produce destructive tsunamis with very short travel times (<10 minutes).

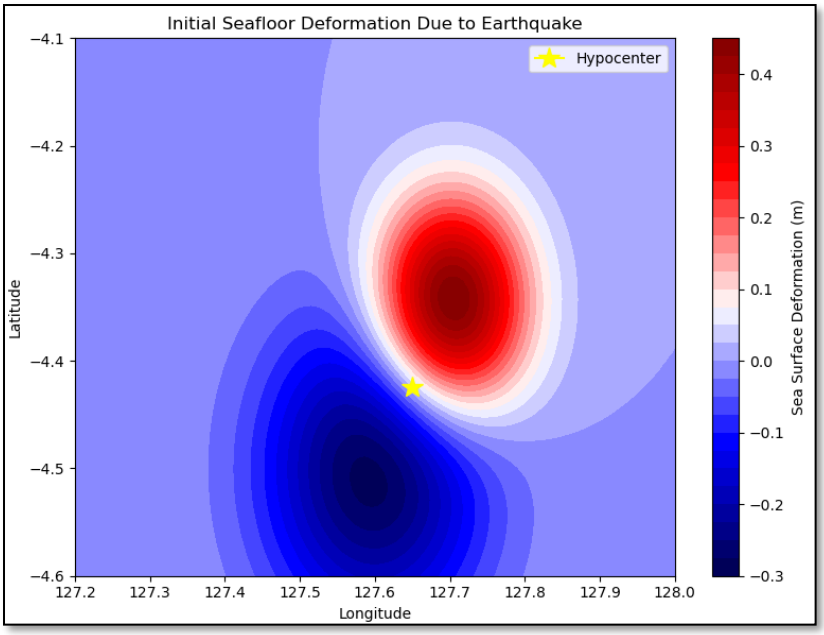


**Figure 4.** Seafloor Deformation Model Generated from an Earthquake Simulation on the South Buru Thrust Fault

Therefore, the deformation model you have constructed is well-founded regarding tsunami generation mechanics. The placement of the hypocenter between the uplift and subsidence regions realistically reflects the location of an active fault zone, and the symmetric distribution of vertical deformation demonstrates sufficient seafloor displacement to initiate a tsunami. Further numerical modelling using COMCOT or other hydrodynamic tools would

be highly valuable in quantifying wave height, arrival times, and inundation with greater precision.

**3D Slip Rate Evolution**

Figure 5 shows the evolution of the 3D slip rate over time on the fault plane of the South Buru Island Earthquake (Mw 8.3), visualized in six panels at 5, 15, 25, 30, 35, and 45 seconds after rupture initiation. From this analysis, it can be seen how the release of seismic energy occurs spatially and temporally and how features such as asperities and segmentation influence the slip rate pattern.

At the initial time (5 seconds), the slip rate is still very low and confined around the epicentre, indicating that the rupture has just begun and has not yet propagated far. By 15 seconds, areas with high slip rates start to develop along the fault plane, particularly toward the western and eastern directions. This indicates the initial phase of radial rupture propagation, a typical pattern also observed in large earthquakes such as the 2011 Tohoku [22]. At 25 and 30 seconds, the slip rate intensity increases sharply, forming two dominant peaks. This phenomenon likely represents the asperity zone, the mechanically stronger part of the fault that stores more energy. When this part fails, a massive release of energy occurs. The presence of two slip rate peaks also indicates that fault segmentation is actively contributing to rupture dynamics, as observed in the 2004 Sumatra-Andaman earthquake, where multi-patch rupture was recorded to trigger tsunami amplification and widespread damage [17],[19],[21].

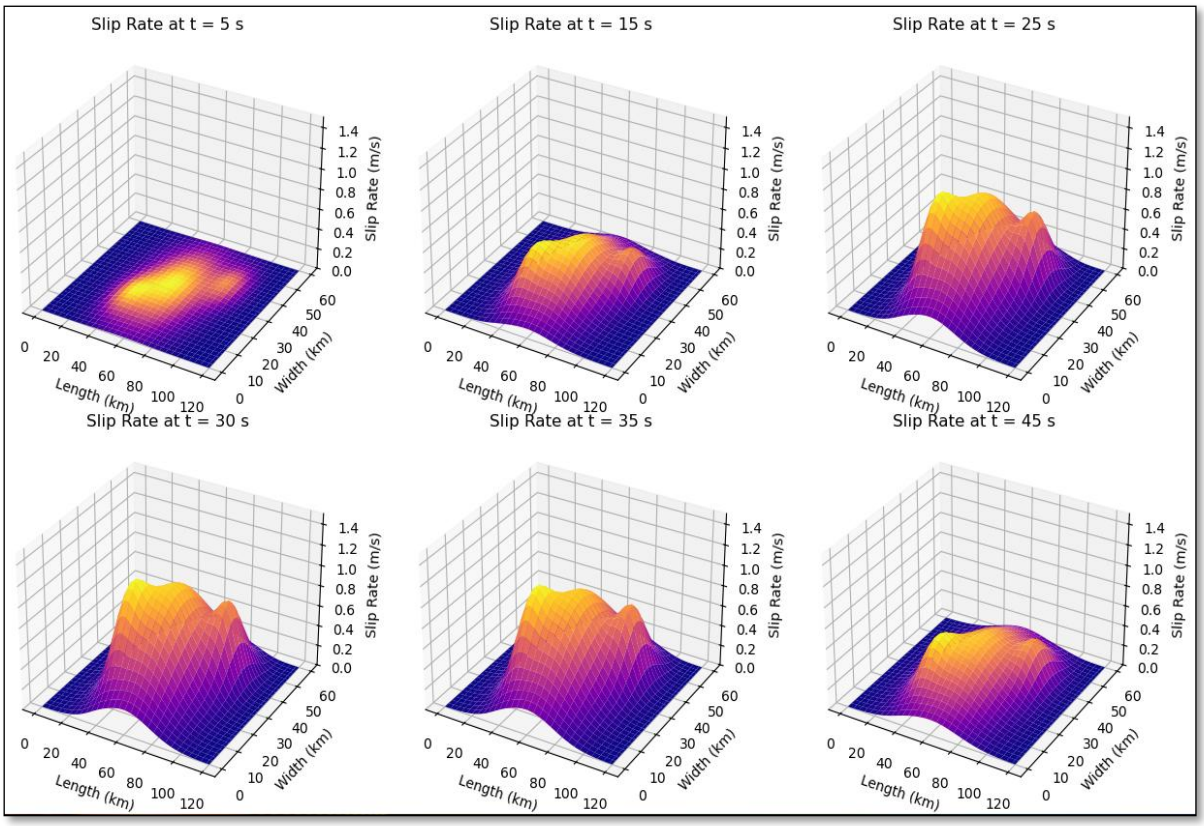


**Figure 5**. 3D Slip Rate Evolution – South Buru Thrust Fault (8.3 Mw)

By 35 to 45 seconds, the rupture had propagated to most of the fault plane area. However, the slip rate decreased, indicating the rupture process was nearing its end. The slip distribution still shows two active zones, reinforcing the hypothesis of segmentation and the presence of dominant asperities. The right side of the fault plane (around x = 90–120 km) shows a lower slip rate throughout the time evolution, consistent with the low-slip segmentation zone explicitly simulated in this model. These findings are consistent with the theory of [24], which states that energy and slip rate evolution are greatly influenced by initial heterogeneous conditions, especially in faults with complex segmentation. Additionally, this simulation approach is similar to the kinematic inversion methodology employed by Minson et al. [25] in the 2010 Chile earthquake model, demonstrating that fault segmentation structure can modulate the rate and distribution of energy release.

This visualization helps understand how rupture propagation, asperity distribution, and segmentation structure influence slip rate evolution in large earthquakes, such as the Southern Buru Island Earthquake. This model supports seismological interpretations of earthquake source complexity, serving as a crucial foundation for earthquake and tsunami risk mitigation efforts in high-risk regions, such as eastern Indonesia.

**Tsunami Run-up Distribution Based on Wave Propagation Modeling from the South Buru Earthquake Source along the Coastal Area of Ambon City**

The South Buru Fault is one of the active tectonic segments in eastern Indonesia, situated within the complex collision zone between the Banda Sea Plate and the island arc system. Geological interpretations and seismotectonic data classify this fault as oblique-slip, striking predominantly in a west-east direction. This study evaluated this fault's earthquake and tsunami potential through numerical modelling, utilizing a hypothetical scenario involving a major earthquake of magnitude Mw 8.3.

This scenario assumes a significant energy release along the fault segment. Although no major tsunamis have historically been attributed to this fault, the potential hazard remains due to the nature of oblique faulting and moderate focal depth, which can generate notable seafloor deformation. Tsunami modelling results indicate possible sea surface uplift near the rupture zone and subsequent tsunami wave propagation toward the coastal areas of Ambon City. The modelled run-up heights vary significantly, depending on the local coastal morphology. This evaluation does not attempt to reconstruct or compare with past tsunami events. Instead, it aims to provide a scientific basis for preparedness and mitigation planning in anticipation of a future megathrust earthquake associated with the South Buru Fault (Figure 6).

The simulation results of tsunami wave propagation triggered by the South Buru Thrust Fault activity demonstrate significant variation in tsunami run-up heights along the coastlines of Ambon Island and its surrounding areas (Figure 7). One of the highest run-up values was recorded at Kapahaha, reaching 13.08 meters, with a wave arrival time of approximately 832 seconds (about 13 minutes and 52 seconds). This suggests that Kapahaha is located very close to the central uplift zone—the area of the fault plane that experienced the most significant vertical displacement due to fault slip. This condition supports the interpretation that the earthquake source is characterized by a dominant asperity in the fault's northwestern segment. The inundated area at Kapahaha was 12,813 $m^2$ with an inundation distance from the shoreline of about 159 meters.

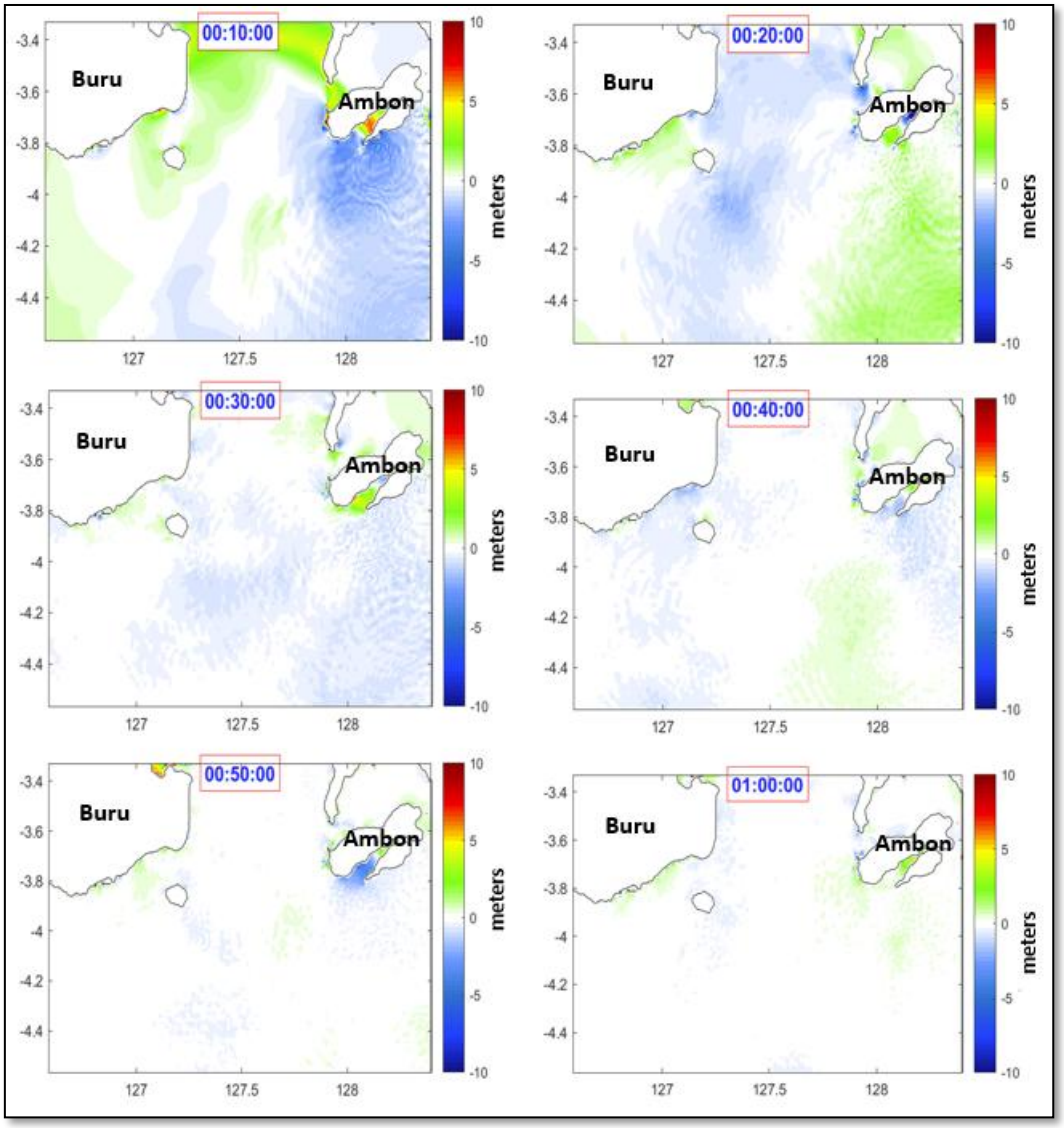


**Figure 6.** Snapshot of the first 60 minutes of tsunami propagation for the South Buru earthquake segment model. Positive wave amplitudes are shown in red, and negative wave amplitudes are shown in blue.

Two other locations, Pasar Mardika and Slamet Riyadi Port, recorded nearly identical run-up heights (12.02 meters) with similar arrival times (786 seconds). This similarity suggests that both sites are located directly within the primary propagation path of waves generated by the maximum slip segment. Additionally, the multi-pulse wave patterns observed at both sites are likely due to resonance and wave reflection within the narrow and shallow harbour areas, which amplify the incoming tsunami waves locally. The inundated area at Mardika was 45,766 m² with an inundation distance from the shoreline of about 217 meters, while at Slamet Riyadi Port, it reached 414,158 m² with an inundation distance of about 1,213 meters.

Yos Sudarso Port and Waiame Dock, which recorded run-up amplitudes of 11.21 meters and 10.68 meters, respectively, also experienced wave arrivals at around 13 minutes, consistent with wave propagation originating from the western part of the fault structure. These similar

characteristics support the hypothesis that the southwestern coastal zone of Ambon serves as a primary energy-receiving region, directly impacted by wave fronts from the area of intense slip release. The inundated area at Yos Sudarso Port was 24,685 m² with an inundation distance from the shoreline of about 168 meters. In comparison, at Waiame Dock, it reached 107,557 m² with an inundation distance of about 246 meters.

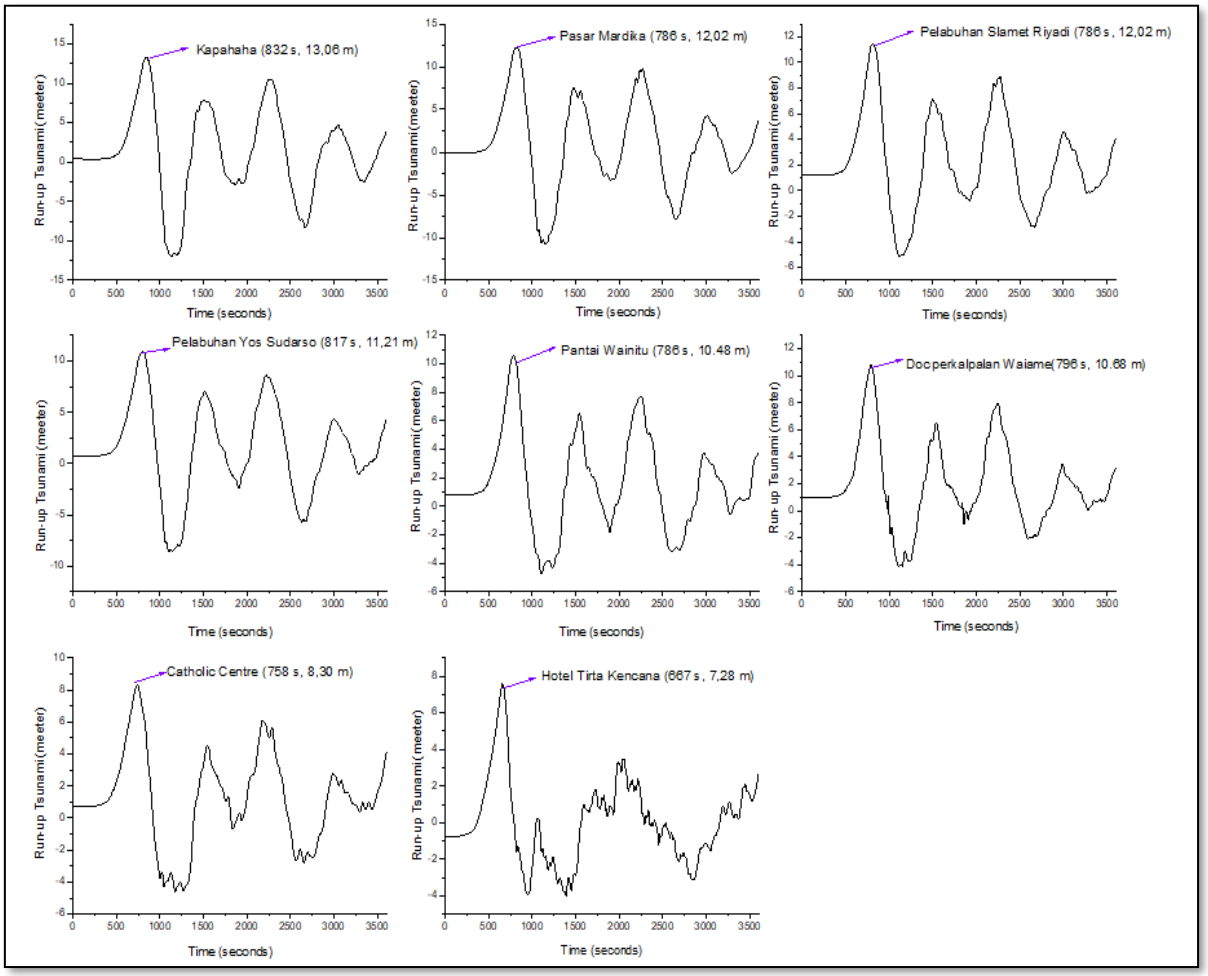


**Figure 7.** Distribution of Tsunami Run-Up along the Coastal Areas of Ambon City

Furthermore, Wainitu Beach recorded a run-up height of 10.48 meters with an arrival time of 786 seconds, indicating an efficient wave propagation path from the earthquake source, which experienced minimal attenuation due to submarine topography. The inundated area at Wainitu Beach was 54,017 m² with an inundation distance from the shoreline of about 383 meters. In contrast, despite registering an earlier wave arrival (758 seconds) with an amplitude of 8.30 meters, the Catholic Centre showed smaller inundation due to its location closer to the lateral extent of the slip segment, where uplift was lower. The inundated area at Catholic Centre was 88,092 m² with an inundation distance from the shoreline of about 206 meters. The site with the earliest wave arrival was Tirta Kencana Hotel (687 seconds, ~11.5 minutes), though it only recorded a run-up of 7.28 meters. The inundated area at Tirta Kencana was 16,580 m² with an inundation distance from the shoreline of about 296 meters.

Overall, the spatial variation in tsunami run-up reflects the complex, segmented nature of the earthquake source. The distribution of wave amplitudes and arrival times is consistent with the 3D slip evolution model, which emphasizes the dominant asperity in the western segment of the fault zone. Local variations in run-up are also influenced by the seafloor topography and coastal morphology, which contribute to wave reflection, focusing, and resonance patterns. In addition, differences in tsunami arrival times can be explained by the combined effects of bathymetry and wave propagation pathways. In deeper waters, tsunami waves travel faster, resulting in shorter arrival times, whereas shallow or complex submarine topography slows wave propagation due to friction, refraction, and scattering. Coastal sites located along the direct propagation path, such as Slamet Riyadi Port and Pasar Mardika, recorded relatively rapid arrivals (~786 seconds), while sites near the lateral extent of the slip or behind bathymetric barriers, such as the Catholic Centre and Tirta Kencana, showed variations with either earlier but weaker arrivals or delayed arrivals due to wave refraction and energy dissipation. These findings underscore the importance of employing a multi-segment rupture model and incorporating 3D deformation analysis to understand tsunamis's spatial impact, particularly in tectonically active archipelagic regions like Ambon.

**Distribution of Tsunami Inundation Impact on Ambon Island**

Based on the results of numerical modelling with an earthquake scenario on the South Buru Fault (Mw 8.3) and raster mapping of tsunami inundation maps (Figure 8), it is evident that the tsunami waves spreading towards Ambon Island experienced energy concentration in several coastal areas. This distribution is significantly influenced by coastal morphology, wave direction, and the presence of bays and capes that can either amplify or block wave propagation.

Latuhalat, located in the southwest part of Ambon Island, has had the most significant impact from the tsunami inundation. Based on a visual interpretation of the map's colour bar (with a colour scale ranging from blue to bright yellow), the inundation height in Latuhalat exceeds 5 meters. This is due to Latuhalat's geographical position, which directly faces the tsunami wave source, and its gently sloping coastal contours, allowing seawater to penetrate deeply into the land.

Additionally, the Galala – Wayame – Laha area also shows high inundation levels, ranging from 3 to 5 meters. This area is a densely populated residential zone near critical infrastructure, including Ambon Port and Pattimura International Airport. The potential disruption to mobility and logistics in this area is significant if a tsunami occurs. For the Paso – Rumah Tiga – Hative Kecil area, tsunami inundation is moderate to high, ranging from 2 to 4 meters deep. Although some parts of the region have slightly higher elevations than the southwest coast, the high population density and economic activity mean the impact still needs to be taken seriously. Meanwhile, the northern and northeastern parts of Ambon Island, such as Lateri, Halong, and Poka, show relatively low inundation heights, generally less than 1 meter. This is due to their more protected location from the primary wave's direction and higher land elevation. However, low-lying coastal areas still require monitoring, especially if there are narrow inlets that could amplify local waves.

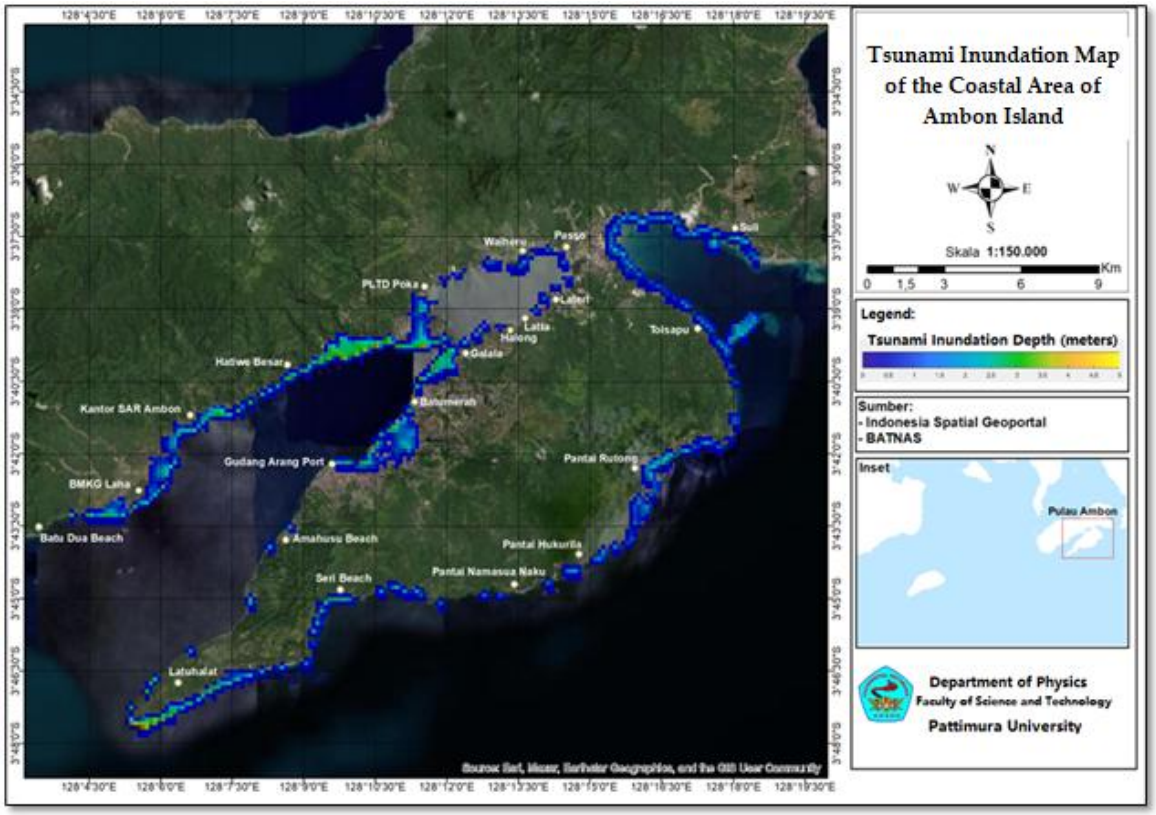


**Figure 8**. Tsunami Inundation Map of the Coastal Area of Ambon Island

**The Importance of Incorporating Non-Subduction Tsunami Sources: A Case Study of the South Buru Thrust Fault**

Numerous global tsunami events over the past decade have underscored the importance of including non-subduction sources, particularly thrust faults, in tsunami hazard assessments. While tsunami mitigation efforts have traditionally focused on large megathrust earthquakes, such as the 2004 Sumatra–Andaman (Mw 9.1) and the 2011 Tohoku (Mw 9.0) events, it is now evident that thrust earthquakes occurring outside the main subduction interface can also generate significant local tsunamis. For instance, the 2021 outer-rise earthquake off the coast of Tonga (Mw 7.4) produced a local tsunami due to vertical seafloor displacement [26], and the 2021 Haiti earthquake (Mw 7.2) similarly triggered a small but locally impactful tsunami [27].

In this study, tsunami simulations using the COMCOT model demonstrate that the South Buru Fault—a thrust fault with a dip angle of 30° and a purely vertical slip component ($\lambda$ = 90°)—has significant potential to generate local tsunamis. Under a scenario involving an Mw 8.3 earthquake with a rupture length of 120 km, a width of 60 km, and a slip displacement of 15 meters, the simulation results indicate tsunami arrival times of less than 14 minutes with maximum run-up heights reaching 13.06 meters along the Kapahaha coast of Ambon. These values suggest the potential inundation of low-lying and densely populated areas. Thrust fault mechanisms of this kind are highly efficient at vertically displacing seawater columns, similar to the Flores Fault earthquakes that previously generated local tsunamis of several meters [28],[29]. These findings are also consistent with the 2018 Sulawesi earthquake (Mw 7.5), which produced tsunami run-up heights of up to 11 meters due to a combination of fault

rupture and submarine landslides [30],[31]. Likewise, analyses of the Flores Fault indicate that regional earthquakes can trigger run-ups of 2–5 meters within less than five minutes, possibly amplified by submarine mass failures [32],[33]. More recent studies further emphasize that thrust faults or fault segments with significant vertical deformation potential can generate tsunamis even when located outside major subduction zones, particularly in eastern Indonesia, where seismic and non-seismic tsunami sources coexist [34],[35].

Therefore, the South Buru Fault should be included in regional tsunami hazard maps and early warning systems. Its offshore location, proximity to the coastline, and capacity for substantial vertical deformation make it a credible and high-potential source of tsunamis. These findings reinforce the urgency of developing tsunami hazard models that more comprehensively account for non-subduction tectonic sources, particularly in geologically complex regions such as eastern Indonesia [36],[37],[38].

## Conclusion

This study assessed the tsunami hazard potential from the South Buru Fault on the coastal areas of Ambon Island. Simulation results indicate that the tsunami arrival time is less than 14 minutes, with a maximum run-up height of 13.06 m at the Kapahaha coast. Among all analyzed locations, Slamet Riyadi Port experienced the greatest impact, with inundation covering an area of 414,158 m² and a penetration distance inland of 1,213 m. This is attributed to its location in a lowland area, with a narrow and shallow bay, and its position directly along the main wave propagation path. Meanwhile, Latuhalat, located in the southwestern part of Ambon Island, experienced the most significant inundation. Based on the visual interpretation of the map colour bar (ranging from blue to bright yellow), inundation heights in Latuhalat reached up to 5 meters. Spatial variations emphasize the role of bathymetry, coastal morphology, and fault segmentation. These results support disaster mitigation, including evacuation planning, early warning systems, and coastal protection, and can be further refined with high-resolution bathymetry, variable slip, and integrated evacuation modelling.

## Acknowledgment

The author would like to express gratitude to the Geophysics Laboratory of Pattimura University for its direct and indirect support throughout the modeling and analysis process. Gratitude is also extended to the Rector of Unpatti and the Dean of the Faculty of Science and Technology for the funding support provided through the Research Grant for Junior Faculty Members, Faculty of Science and Technology, Year 2025, as per Rector's Decision No. 1248/UN13/SK/2025.

## References

[1] R. Hall, "Cenozoic geological and plate tectonic evolution of SE Asia and the SW Pacific: computer-based reconstructions, model and animations," *Journal of Asian Earth Sciences*, vol. 39, no. 4, pp. 229–244, 2012.

[2] Y. Tanioka and K. Satake, "Tsunami generation by horizontal displacement of ocean bottom," *Geophysical Research Letters*, vol. 23, no. 8, pp. 861–864, 1996.

[3] C. J. Westen, "Local tsunami early warning systems in the context of risk management," *Journal of Disaster Research*, vol. 6, no. 2, pp. 104–113, 2011

[4] S. L. Soloviev and C. N. Go, *Catalogue of Tsunamis on the Western Shore of the Pacific Ocean*. Canada: Canadian Translation of Fisheries and Aquatic Sciences, no. 5078, 1984, 310 p, 1984.
[5] BMKG, "Gempa Bumi 5.0 SR Laut Banda, 2 Oktober 2023," *Badan Meteorologi, Klimatologi, dan Geofisika*, Jakarta, 2023. [Online]. Available: https://www.bmkg.go.id. [Accessed June 28, 2025].
[6] D. Renaldi, P. Wijayanti, and A. Fitriyani, "Analisis risiko tsunami di wilayah pesisir Ambon menggunakan metode multi-criteria analysis," *Jurnal Geografi*, vol. 20, no. 1, pp. 55–66, 2023.
[7] T. Arikawa, K. Shimosako, T. Tomita, T. Takabatake, and M. Esteban, "Characteristics of tsunami propagation and inundation in Onagawa Bay due to the 2011 Tohoku earthquake," *Coastal Engineering Journal*, vol. 61, no. 1, pp. 31–52, 2019.
[8] I. R. Pranantyo and P. R. Cummins, "The 1674 Ambon tsunami: Extreme run-up caused by an earthquake-triggered landslide," *Pure and Applied Geophysics*, vol. 177, no. 5, pp. 1641–1656, 2020.
[9] L. Shao, Y. Yu, Y. Cheng, and J. Zhang, "Numerical simulation of tsunami wave run-up in different coastal topographies," *Natural Hazards*, vol. 107, pp. 2143–2163, 2021.
[10] H. Yeh, I. N. Robertson, and J. Preuss, "Development of tsunami-resilient communities," *Earthquake Spectra*, vol. 21, no. S1, pp. 367–371, 2005.
[11] M. J. Briggs, C. E. Synolakis, G. S. Harkins, and D. R. Green, "Laboratory experiments of tsunami run-up on a circular island," *Pure and Applied Geophysics*, vol. 144, no. 3–4, pp. 569–593, 1995.
[12] R. Hidayat, J. Sopaheluwakan, and A. D. Nugraha, "Tsunami hazard assessment in Banda Sea region," *Journal of Disaster Research*, vol. 15, no. 7, pp. 972–981, 2020.
[13] A. R. Gusman, K. Satake, and K. Goda, "Probabilistic tsunami hazard in Indonesia due to active fault sources," *Pure and Applied Geophysics*, vol. 179, no. 2, pp. 677–698, 2022.
[14] Y. Noya, I. Meilano, I. Pranantyo et al., "Tsunami threat from the Seram Fault system," *Natural Hazards and Earth System Sciences*, vol. 23, pp. 943–958, 2023.
[15] P. L.-F. Liu, S. B. Woo, and Y. S. Cho, *Computer programs for tsunami propagation and inundation*, Ithaca, NY: Cornell University, no. 98-01, 1998, 85 p, 1998.
[16] X. Wang, *COMCOT User Manual Version 1.7*, Ithaca, NY: Cornell University, 37 p, 2009.
[17] K. Kajiura dan N. Shuto, "Tsunami numerical simulation," in *Handbook of Coastal Disaster Mitigation for Engineers and Planners*, Tokyo: University of Tokyo Press, pp. 151–166, 1990.
[18] L. Li, X. Deng, and H. Liu, "Numerical simulation of tsunami inundation with varying bottom friction," *Natural Hazards and Earth System Sciences*, vol. 13, no. 11, pp. 2835–2848, 2013.
[19] G. S. Prasetya, T. M. Wilson, and W. L. Power, "Tsunami modeling for local sources in Indonesia," *Natural Hazards and Earth System Sciences*, vol. 11, no. 12, pp. 3233–3246, 2011.
[20] T. Lay, H. Kanamori, C. J. Ammon, M. Nettles, S. N. Ward, R. C. Aster *et al*., "The great Sumatra–Andaman earthquake of 26 December 2004," *Science*, vol. 308, no. 5725, pp. 1127–1133, 2005.
[21] E. A. Okal, "Tectonic settings of historic and modern tsunamigenic earthquakes in the eastern Mediterranean Sea," *Pure and Applied Geophysics*, vol. 160, pp. 1917–1951, 2003.
[22] [22] K. Satake (ed.), *Tsunamis: Case Studies and Recent Developments*, *Advances in Natural and Technological Hazards Research*, vol. 23, Dordrecht/New York: Springer, 2005.
[23] E. L. Geist and T. Parsons, "Tsunami generation by thrust faulting offshore," *Journal of Geophysical Research*, vol. 110, B4, B04307, 2005.

[24] R. C. Viesca and D. I. Garagash, "Ubiquitous weakening of faults by stress-driven fluid flow," *Nature Geoscience*, vol. 8, no. 11, pp. 875–879, 2015.
[25] S. E. Minson, M. Simons, J. L. Beck et al., "Bayesian inversion for finite fault earthquake source models using near-field and far-field seismic and geodetic data," *Journal of Geophysical Research: Solid Earth*, vol. 119, no. 11, pp. 8288–8315, 2014.
[26] M. Heidarzadeh, T. Ishibe, O. Sandanbata, A. Muhari, dan A. B. Wijanarto, "The 29 August 2021 Mw 7.4 earthquake in the Kermadec–Tonga region: insights on tsunami generation from outer-rise earthquakes," *Pure and Applied Geophysics*, vol. 179, no. 5, pp. 1983–1997, 2022.
[27] H. M. Fritz, F. Mohammed, E. A. Okal, and C. E. Synolakis, "Field survey of the August 14, 2021 tsunami in Haiti," *Pure and Applied Geophysics*, vol. 179, no. 3, pp. 1111–1127, 2022.
[28] F. H. Nguyen, A. R. Gusman, K. Satake, and S. Watada, "Tsunami modeling of the 1992 Flores, Indonesia earthquake using updated bathymetric and seismic data," *Journal of Geophysical Research: Solid Earth*, vol. 127, no. 2, e2021JB023235, 2022.
[29] R. M. W. Musson, F. I. Gonzalez, S. Lorito et al., "A review of local tsunami hazard assessments in complex tectonic regions," *Natural Hazards and Earth System Sciences*, vol. 19, no. 4, pp. 911–930, 2019.
[30] M. Carvajal, S. A. Sepúlveda, and J. S. Haase, "Insights on the 2018 Sulawesi tsunami in Palu, Indonesia: A complex event due to co-seismic landslide and fault rupture," *Scientific Reports*, vol. 9, no. 1, 11920, 2019.
[31] S. Widiyantoro, S. Rosalia, T. Zulhan, P. Supendi, I. R. Pranantyo, A. D. Nugraha et al., "The 2018 Palu–Sulawesi earthquake and tsunami: insights from tsunami numerical modeling," *Geoscience Letters*, vol. 7, no. 1, 11, 2020.
[32] B. K. Rastogi and R. K. Jaiswal, "A catalog of tsunamis in the Indian Ocean," *Science of Tsunami Hazards*, vol. 24, no. 3, pp. 58–88, 2006.
[33] I. H. Pranantyo, A. R. Gusman, and K. Satake, "Possible landslide source of the 1992 tsunami in Flores Island, Indonesia," *Natural Hazards and Earth System Sciences*, vol. 22, no. 3, pp. 777–792, 2022.
[34] S. Widiyantoro, I. Meilano, I. R. Pranantyo, and P. R. Cummins, "Complex tsunami hazards in eastern Indonesia from seismic and non-seismic sources: deterministic modelling based on historical and modern data," *Geoscience Letters*, vol. 8, no. 20, 2021.
[35] J. Paskett, D. Melgar, A. L. Williamson, et al., "High tsunamigenic potential of crustal faults with vertical displacement," *Geophysical Research Letters*, vol. 50, no. 6, e2022GL101503, 2023.
[36] B. D. Mutaqin, E. Kriswati, and S. Hidayati, "Tsunami hazard zoning and exposure mapping using a GIS-based multicriteria approach in eastern Indonesia," *International Journal of Disaster Risk Reduction*, vol. 35, 101065, 2019.
[37] Badan Meteorologi, Klimatologi, dan Geofisika (BMKG), Peta Sumber dan Bahaya Gempa Indonesia 2021. Jakarta: BMKG, 2021. [Online]. Available: https://www.bmkg.go.id/gempabumi/gempabumi-terkini.bmkg. [Accessed June 29, 2025].
[38] A. R. Gusman, S. Murotani, K. Satake, and M. Heidarzadeh, "Tsunami source of the 2019 Ambon, Indonesia earthquake," *Geophysical Research Letters*, vol. 49, no. 8, e2021GL097457, 2022.